

# A way of resolving the order-of-limit problem of Tao-Mo semilocal functional

Abhilash Patra,<sup>1,\*</sup> Subrata Jana,<sup>1,†</sup> and Prasanjit Samal<sup>1,‡</sup>

<sup>1</sup>*School of Physical Sciences, National Institute of Science Education and Research, HBNI, Bhubaneswar 752050, India*

(Dated: August 14, 2020)

It is highlighted recently that the Tao-Mo (TM) [Phys. Rev. Lett. **117**, 073001 (2016)] semilocal exchange-correlation energy functional suffers from the order-of-limit problem, which affects the functional performance for phase transition pressures [J. Chem. Phys. **152**, 244112 (2020)]. The root of the order-of-limit problem of the TM functional inherent within the interpolation function, which switches between the compact density and the slowly varying density. In this paper, we propose a different switch function that avoids the order-of-limit problem and interpolates correctly between the compact density and the slowly varying fourth-order density correction. By circumventing the order-of-limit problem, the proposed form enhances the applicability of the original TM functional on the diverse nature of the solid-state properties. Our conclusion is ensured by examining the functional in predicting properties related to the general-purpose solids, quantum chemistry, and phase transition pressure. Besides, we reasonably discuss the connection between the order-of-limit problem, phase transition pressure, and band gap of solids.

## I. INTRODUCTION

The Kohn-Sham formalism of the density functional theory [1, 2] is the *de facto* standard for performing the electronic structure calculation of the atoms, molecules, solids, and clusters. While the theory is exact, the accuracy of DFT depends on the approximations of the exchange-correlation (XC) functionals having all the many-body effects. The development of efficient yet accurate XC functionals is an emerging topic in DFT for the last couple of decades and continues to be the same. Encouraging approximations have been proposed in different levels, such as local density approximation (LDA) [3], generalized gradient approximation (GGA) [4–17], meta-GGA [18–38], (screened-)hybrid density functional [39–42], and double-hybrid density functionals [43], to improve the electronic structure calculations of solids and quantum chemical systems. However, within the different rungs of the approximations, the semilocal form of the XC approximations (LDA, GGA, and meta-GGA), proposed by satisfying exact constraints, are most common for the solid-state physics and quantum chemistry. In the semilocal levels, the meta-GGA functionals are the advanced and (more) accurate one for the solid-state and chemical calculations [44–56] which is written as,

$$E_{xc}^{meta-GGA} = \int \rho(\mathbf{r}) \epsilon_x^{LDA} F_{xc}^{meta-GGA}(\rho, \nabla\rho, \nabla^2\rho, \tau), \quad (1)$$

where,  $\epsilon_x^{LDA}$  is the LDA exchange functional,  $\rho, \nabla\rho, \nabla^2\rho, \tau$  are the density, gradient of density, Laplacian of density, and KS kinetic energy density, respectively. Due to the dependence of the KS kinetic energy and other built-in ingredients, the meta-GGA functionals recognize the single, overlap, and slowly

varying density region in a much better way than GGA does [54]. However, in DFT it is a common practice to construct more accurate semilocal XC by getting rid of the deficiencies of the proposed XC functionals.

Recent advances in the development of the semilocal functionals demonstrate that more accurate density functionals can be proposed by satisfying as much as quantum mechanical constraints. One of the most important development came through the strongly constrained and appropriately normed (SCAN) [26] meta-GGA functional, which is quite an accurate functional for the diverse nature of the solid-state and molecular properties [57]. Several modifications of the SCAN functional are also proposed. Besides the SCAN functional, the recently proposed Tao-Mo (TM) [28] functional is also showing promising performance for finite and extended systems [45, 48, 51, 52]. Besides, the built-in exchange hole of the TM functional extended to construct the range-separated hybrid density functionals for finite and extended systems [58–61]. Also, a revision of the TM functionals (revTM) is proposed very recently [36]. Importantly, the TM based functionals correctly satisfy two important paradigms, one- or two-electron limit, important for quantum chemistry and the slowly varying fourth-order density gradient approximation, relevant to condensed matter physics. However, both the TM and revTM functionals suffer from the order-of-limit problem anomaly, which is an important limitation and degrades its performance for the transition pressure solids [62]. The order-of-limit problem of the meta-GGA functionals come from the iso-orbital indicator  $z = \tau^W/\tau = 1/(1+(3/5)(\alpha/p))$ , where  $\alpha = \frac{\tau - \tau^W}{\tau^{unif}}$  is another iso-orbital indicator, also known as Pauli kinetic energy density. Here,  $p(= s^2 = \frac{|\nabla\rho|^2}{(4k_F\rho)^2})$ ,  $\tau$ ,  $\tau^W$ , and  $\tau^{unif}$  are the square of the reduced density gradient  $s$ , KS, von Weizsacker, and uniform kinetic energy density, respectively. In the limit of vanishing  $\alpha$  and  $p$  limit

\* abhilashpatra@niser.ac.in

† subrata.jana@niser.ac.in, subrata.niser@gmail.com

‡ psamal@niser.ac.in

the order-of-limit problem occurs as [27, 63],

$$\lim_{p \rightarrow 0} \left[ \lim_{\alpha \rightarrow 0} \frac{1}{1 + \frac{3\alpha}{5p}} \right] = 1. \quad (2)$$

while

$$\lim_{\alpha \rightarrow 0} \left[ \lim_{p \rightarrow 0} \frac{1}{1 + \frac{3\alpha}{5p}} \right] = 0. \quad (3)$$

In the main paper of the TM functional [28], the problem has been overlooked with statement ‘‘this only happens near a nucleus’’. However, it is shown recently [32] that the existence of this problem deteriorates the functional performance for the transition pressure of solids. Although the order-of-limit problem does not seem to be an important restriction for non-covalent ( $\alpha \gg 1$ ) and slowly varying density region ( $\alpha \approx 1$ ), but it seems to be a significant limitation for the center of the single-bonded region formed in molecules or solids. Also, during the change of the phases of two solids, where the formation of bonding and energy differences are important. Hence, during the meta-GGA functional construction, the order-of-limit problem must be taken into account. Note that TPSS and its revised version (revTPSS) also suffer from the order-of-limit anomaly, which is resolved by regularizing the functionals known as the regTPSS functional [27]. Recent meta-GGAs like meta-GGA made simple (MS1, MS2, and MVS) and SCAN functionals do not have any order-of-limit problem because those are constructed using meta-GGA ingredient  $\alpha$ .

To find a way to resolve the order-of-limit problem of the TM functional (which, we named as regularized Tao-Mo (regTM) functional), in this paper, we propose a slightly different form of the iso-orbital indicator  $z$ . Our resolution is described by arranging the paper as follows: In the next section, we will briefly describe the TM functional and its order-of-limit problem. A possible way to resolve the order-of-limit problem of the TM functional is also discussed in that section. Following this, we demonstrate the functional performance by assessing it for general purpose solids, molecules, and transition pressure problems.

## II. THEORY

To start, we first consider the functional form of the Tao-Mo (TM) functional and the underlying problems associated with it. The exchange enhancement factor of the TM functional is given by [28],

$$F_x^{TM}(p, z, \alpha) = w F_x^{DME} + (1 - w) F_x^{sc}, \quad (4)$$

where

$$F_x^{DME}(p, \alpha) = \frac{1}{f^2} + \frac{7R}{9f^4} \quad (5)$$

with  $R = 1 + 595(2\lambda - 1)^2 \frac{p}{54} - [z_3 - 3(\lambda^2 - \lambda + 1/2)(z_3 - 1 - z_2/9)]$  and  $f = [1 + 10(70y/27) + \beta y^2]^1/10$ . Here,  $z_2 =$

$\tau^W/\tau^{unif} = 5p/3$ ,  $z_3 = \tau/\tau^{unif} = z_2 + \alpha$ ,  $y = (2\lambda - 1)^2 p$ ,  $\tau^{VW} = |\nabla\rho|^2/(8\rho)$ , and  $\tau^{unif} = \frac{3}{10}(3\pi^2)^{2/3}\rho^{5/3}$ . The slowly varying correction part of the enhancement factor given as [28],

$$F_x^{sc}(p, \alpha) = \left\{ 1 + 10 \left[ \left( \frac{10}{81} + \frac{50}{729} p \right) p + \frac{146}{2025} q^2 - \frac{73}{405} q \frac{3z}{5} (1 - z) \right] \right\}^{1/10}. \quad (6)$$

where,  $z = \tau^W/\tau = 5p/(5p + 3\alpha)$  and  $w = (z^2 + 3z^3)/(1 + z^3)^2$ . The order-of-limit problem of the TM exchange enhancement factor arises from the order of two limiting conditions  $p \rightarrow 0$ , and  $\alpha \rightarrow 0$ . The discontinuity in the enhancement factor observed with,

$$\lim_{\alpha \rightarrow 0} \left[ \lim_{p \rightarrow 0} [F_x^{TM}(p, \alpha)] \right] = 1.01372, \quad (7)$$

and

$$\lim_{p \rightarrow 0} \left[ \lim_{\alpha \rightarrow 0} [F_x^{TM}(p, \alpha)] \right] = 1.1132. \quad (8)$$

However, it is observed that none of the  $F_x^{DME}(p, \alpha)$  and  $F_x^{sc}(p, \alpha)$  face any order-of-limit problem,

$$\lim_{p \rightarrow 0} \left[ \lim_{\alpha \rightarrow 0} [F_x^{DME}(p, \alpha)] \right] = \lim_{\alpha \rightarrow 0} \left[ \lim_{p \rightarrow 0} [F_x^{DME}(p, \alpha)] \right] = 1.1132 \quad (9)$$

and

$$\lim_{p \rightarrow 0} \left[ \lim_{\alpha \rightarrow 0} [F_x^{sc}(p, \alpha)] \right] = \lim_{\alpha \rightarrow 0} \left[ \lim_{p \rightarrow 0} [F_x^{sc}(p, \alpha)] \right] = 1.01372. \quad (10)$$

The iso-orbital indicator  $z$  present in the weight factor of Eq. 4 is the root cause of the order-of-limit problem.

In search for appropriate weight factor, we propose modified iso-orbital indicator ( $z'$ ) as,

$$z' = \frac{1}{1 + \left(\frac{3}{5}\right) \left[ \frac{\alpha}{p + f(\alpha, p)} \right]}, \quad (11)$$

where, the function  $f(\alpha, p)$  is considered as proposed in ref. [27] as  $f(\alpha, p) = \frac{(1-\alpha)^3}{(1+(d\alpha)^2)^{3/2}} e^{-cp}$  with  $d = 1.475$  and  $c = 3.0$ . This choice of the iso-orbital indicator lifts the order-of-limit problem as,

$$\lim_{p \rightarrow 0} \left[ \lim_{\alpha \rightarrow 0} [z'] \right] = \lim_{\alpha \rightarrow 0} \left[ \lim_{p \rightarrow 0} [z'] \right] = 1. \quad (12)$$

Note that any small positive definite quantity or real number instead of  $f(\alpha, p)$  can remove the order-of-limit problem of  $z'$ . However, the present choice of  $z'$  keeps the exchange enhancement factor close to that of the TM functional (except  $s, \alpha \rightarrow 0$ ), which is important. In ref. [27], the functional  $f(\alpha, p)$  is considered to interpolation between  $\alpha = 0$  and ordinary  $\alpha$  values. But in the present case,  $f(\alpha, p)$  is added to the square of the reduced density gradient ( $p$ ) such that the function  $\frac{\alpha}{p}$  becomes a finite number even for  $p = 0$ , and a finite  $\alpha$ . We keep the

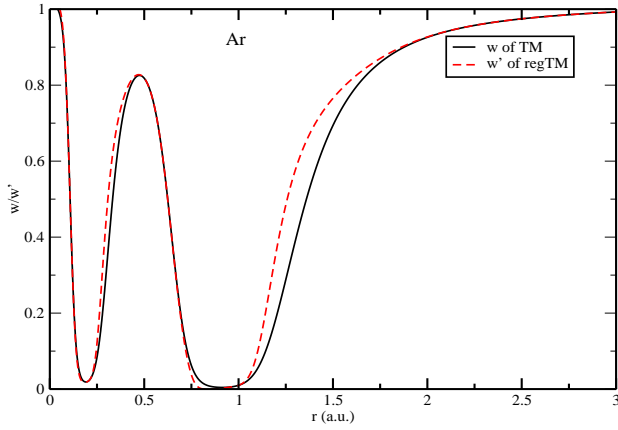


FIG. 1. Shown is the  $w$  of TM ( $w'$  of regTM) for the Ar atom along the radial distance from the nucleus  $r$ .

original values of  $c$  and  $d$  as mentioned in ref. [27], since the order-of-limit is important only for  $s \rightarrow 0$  and  $\alpha \rightarrow 0$ . Whereas, for other values of  $s$  and  $\alpha$ , the regTM exchange enhancement factor matches smoothly with that of TM to keep the accuracy of the original functional.

With the modified iso-orbital indicator the weight factor of the TM functional becomes,

$$w' = \frac{z'^2 + 3z'^3}{(1 + z'^3)^2}. \quad (13)$$

For one or two-electron singlet state,  $\alpha = 0$ , that implies  $z' = 1$ ,  $w' = 1$ , and  $F_x^{regTM} = F_x^{DME}$ . For slowly varying density region,  $\alpha \approx 1$ ,  $f(\alpha, p) \approx 0$  and  $w'$  is small. Hence,  $F_x^{sc}$  is the dominating term that is necessary for solids. For non-covalent bonding,  $\alpha \gg 1$ ,  $f(\alpha, p)$  is small except for small  $s$ . For example,  $\alpha = 10$ ,  $f(10, p)$  is zero for  $s > 1.6$ . The form of  $f(\alpha, p)$  is such that  $F_x^{regTM}$  matches closely with that of the  $F_x^{TM}$  for different  $\alpha$  and  $s$  values except for those two limiting values from which order-of-limit occurs. Keeping the  $F_x^{regTM}$  close to the  $F_x^{TM}$  is important because  $F_x^{TM}$  is a quite good functional for weakly bonded systems and strongly bound solids, including the non-covalent interactions and layered materials. Other forms of the  $w'$  can be proposed based on the different iso-orbital indicators like  $\alpha$  and  $\beta$  [32], but those may make the functional behavior quite different from  $F_x^{TM}$ , especially, for large  $\alpha$ , which is important for non-covalent systems [54, 64]. For  $\alpha = 0$ ,  $F_x^{TM}$  and  $F_x^{regTM}$  reduce to  $F_x^{DME}$  and for all values of  $\alpha$ . For comparison, in Fig 1, we plot the  $w$  and  $w'$  for TM and regTM functional for Ar atom along the radial distance ( $r$ ) from the nucleus. Both the  $w$  and  $w'$  match for the near nucleus and tail region ( $\alpha \approx 1$ ). In the middle of the inter-shell region only slight difference is observed between these two curves indicating the consistency of the both  $w$  and  $w'$  by construction.

Now, the use of  $w'$  in Eq. 4 lifts the order-of-limit

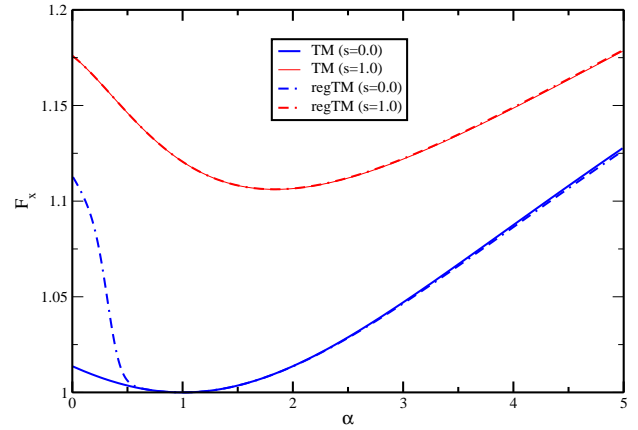


FIG. 2. The difference in the enhancement factor of TM and regTM with the variation of  $\alpha$  for particular values of  $s$  are shown. For  $s = 0$ , the drastic difference at  $\alpha = 0$  is clearly from the correction of order-of-limit problem

problem and follows,

$$\lim_{p \rightarrow 0} [\lim_{\alpha \rightarrow 0} [F_x^{regTM}(p, \alpha)]] = \lim_{\alpha \rightarrow 0} [\lim_{p \rightarrow 0} [F_x^{regTM}(p, \alpha)]] = 1.1132 \quad (14)$$

In Fig. 2, we compare the variation in the enhancement factors of both TM and regTM exchange functionals with  $\alpha$ , and a particular value of  $s$ . The order-of-limit correction is clear at  $\alpha = 0$  for  $s = 0$  curves. For other values of  $\alpha$  and  $s$ , the regTM exchange enhancement factor matches very closely with that of the TM functional.

Regarding correlation, we consider the regTPSS correlation energy functional [27]. The regTPSS correlation functional is also utilized with MS1, MS2, and MVS functionals, and it seems to be more suitable for functionals proposed by removing the order of limit problem. The use of TM or TPSS correlation energy functional does not work well with the regTM functional as the obtained AE6 atomization energies are  $\approx 8.0$  kcal/mol. The only price the regTPSS correlation pays is that it is not one-electron self-correlation free, which is important for molecules having many H atoms, such as water clusters. But as stated in ref. [27], molecular reaction energies do not influence much by the atomic energy errors, and it depends on the error cancellation effects obtained from exchange and correlation. Also, the spin-independent of the XC functional for  $0 < \zeta < 0.7$  [26, 63], a constraint, important for improving the atomization energies, which TM XC functional respects well (see Fig. 2 of ref. [28]).

### III. RESULTS AND DISCUSSIONS

#### A. General assessment

To assess the regTM functional performance along with TM functional, we consider general-purpose quantum chemical and solid-state test sets. For quantum

TABLE I. Tabulated are the mean absolute errors for molecular (main group thermochemistry, barrier heights and non-covalent interactions) and solid-state (equilibrium lattice constants, bulk moduli, and cohesive energies of a set of 29 bulk materials) tests. Best values within TM and regTM are marked with bold style. The zero-point an-harmonic expansion (ZPAE) corrected reference values for lattice constants, bulk moduli, and cohesive energies are taken from ref. [36, 46, 49]. For LC20, BM20, and COH20 test sets are taken from refs. [27, 49].

	TM	regTM
Molecular tests		
Main group thermochemistry (kcal/mol)		
AE6	4.5	<b>4.4</b>
G2/148	6.5	<b>5.7</b>
IP13	<b>3.17</b>	3.76
EA13	3.79	<b>3.25</b>
PA8	<b>2.13</b>	5.13
Barrier heights (kcal/mol)		
BH6	7.59	<b>5.47</b>
HTBH38	7.25	<b>7.17</b>
NHTBH38	8.86	<b>8.29</b>
Non-covalent interactions (kcal/mol)		
HB6	0.23	<b>0.10</b>
DI6	0.40	<b>0.30</b>
CT7	2.87	<b>2.67</b>
PPS5	0.74	<b>0.62</b>
WI7	<b>0.04</b>	<b>0.04</b>
S22	0.61	<b>0.55</b>
WATER27	<b>1.44</b>	1.53
TMAE	3.34	<b>3.26</b>
Solid-State tests		
Lattice constants (Å)		
simple metals	0.051	<b>0.044</b>
transition metals	<b>0.024</b>	0.026
ionic solids	0.039	<b>0.037</b>
semiconductors and insulators	<b>0.015</b>	0.028
total MAE	<b>0.033</b>	0.034
LC20	<b>0.032</b>	0.033
bulk moduli (GPa)		
simple metals	1.5	<b>1.1</b>
transition metals	<b>9.9</b>	<b>9.9</b>
ionic solids	<b>4.2</b>	4.4
semiconductors and insulators	6.4	<b>6.1</b>
total MAE	5.5	<b>5.3</b>
BM20	4.2	<b>3.8</b>
cohesive energies (eV)		
simple metals	0.274	<b>0.155</b>
transition metals	0.751	<b>0.570</b>
ionic solids	<b>0.069</b>	0.095
semiconductors and insulators	0.122	<b>0.078</b>
total MAE	0.304	<b>0.224</b>
COH20	0.282	<b>0.216</b>

chemistry, the Minnesota 2.0 [68] is considered except G2/148 (atomization energies of 148 molecules), S22 (22 non-covalent interactions), and WATER27 test sets [69, 70]. The G2/148 test set is considered from ref. [71], whereas geometries of S22 and WATER27 are taken from GMTKN55 [72]. Overall, the test set is divided into the main group thermochemistry, barrier heights, and non-covalent interactions. The thermochemistry group consists of (1) AE6 - atomization energies of 6 molecules [73], (2) G2/148 - atomization energies of 148 molecules [71], (3) EA13 - 13 electron affinities [68], (4) IP13 - 13 ionization potentials [68], and (5) PA8 - 8 proton affinities [68]. The barrier height test set consists with: (1) BH6 - 6

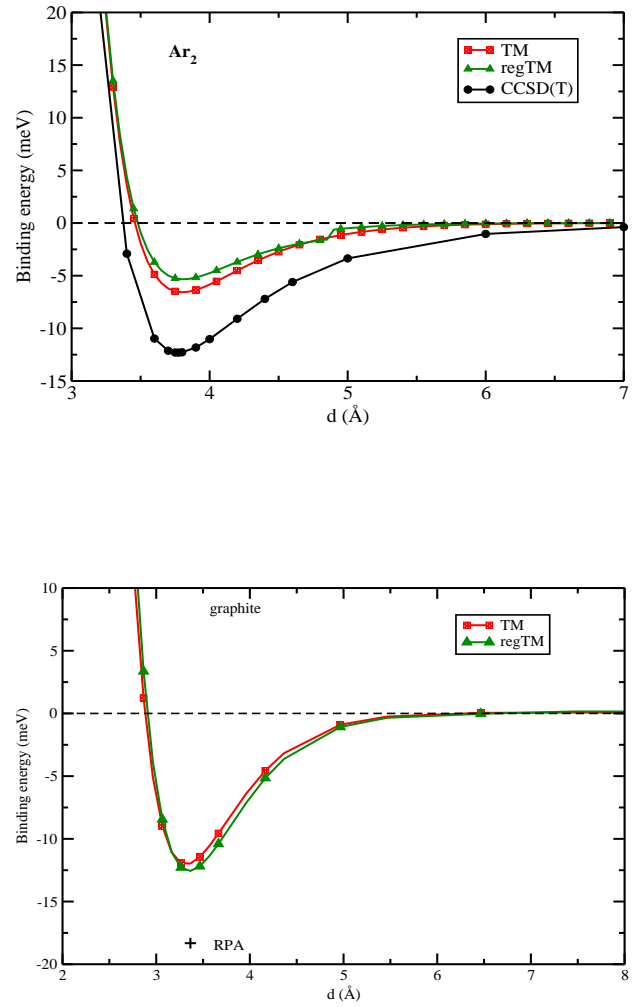


FIG. 3. The binding energy curve of the  $\text{Ar}_2$  dimer (upper panel) and graphite (lower panel) as obtained from TM and regTM functionals. The CCSD(T) and RPA values are taken from ref. [65, 66] and ref. [67] respectively.

barrier heights [73], (2) HTBH38 - 38 hydrogen barrier heights [74], and (3) NHTBH38 - 38 non-hydrogen barrier heights [74]. For the non-covalent group we consider: (1) HB6 - 6 hydrogen bond test set [75], (2) DI6 - 6 dipole interactions [75], (3) CT7 - 7 charge transfer molecules [75], (4) PPS5 - binding energies of five  $\pi - \pi$  stacking complexes [75], (5) WI7 - 7 weekly interaction complexes [75], and (4) S22 - 22 non-covalent interaction molecules including H-bond, dispersion interactions, and mixed bonds [76, 77], and (5) WATER27 - 27 water cluster binding energies [69, 70].

The performance of the TM and regTM functionals for the molecular test cases are summarized in Table I. Regarding the performance, both functionals behave equivalently for main group thermochemistry except for PA8, for which the regTM worse than TM. For barrier height, regTM performs slightly better than TM both for the hydrogen and non-hydrogen transfer barrier heights. Importantly, the resolution of the order-of-limit problem

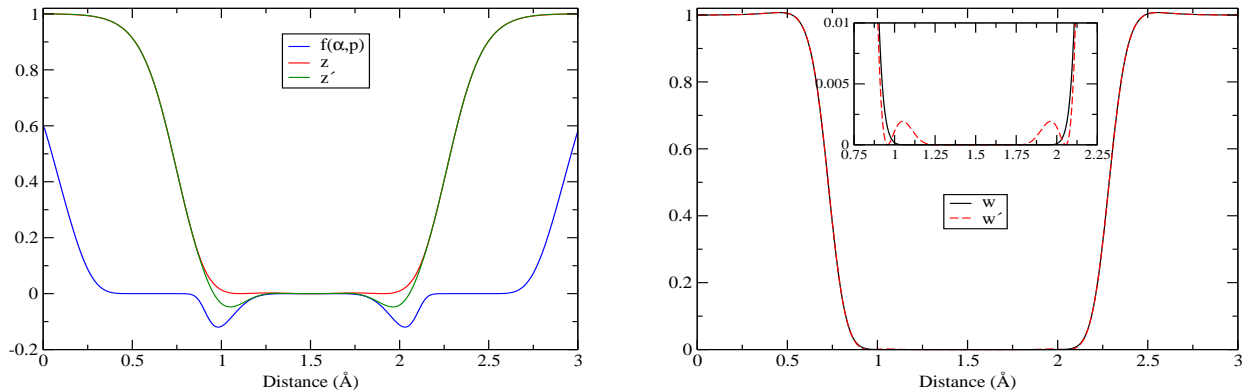


FIG. 4. Shown are the different meta-GGA ingredients and interpolation functions for Li from the atom at  $(0, 0, 0)$  to  $(1/2, 1/2, 1/2)$ . Left panel showing  $f(\alpha, p)$ ,  $z$ , and  $z'$ . Right panel showing  $w$  and  $w'$ .

seems important for the barrier height [27]. Interesting results are also observed for H-bond and non-covalent interactions. Regarding the performance, regTM produces a slightly better result than TM for H-bonded, dipole interactions, charge transfer, and  $\pi - \pi$  stacking complexes. The improvement for H-bonds for regTM functional is also reflected in the performance of the S22 test set, where regTM is overall better than TM functional for H-bonded and mixed complexes. We observe that for non-covalent interactions, especially for H-bonded systems, regTM binding energies are slightly lower than the TM functional, making binding energies closer to the experimental values. However, this moderate underestimation causes slightly worse performance of regTM for 27 water clusters binding energies than TM functional. This behavior of the regTM functional for non-covalent interaction may happen because  $F_x^{regTM}$  slightly enhanced than  $F_x^{TM}$  (coming from  $f(\alpha, p)$  function) for  $\alpha \gg 1$ , important for the non-covalent interaction. Also, one can not rule out the lack of one-electron self-interaction free correlation for regTM, which may also be responsible for the error cancellation between exchange and correlation.

Next, we turn into the solid-state performance of the functionals. For solids the recovery of the slowly varying fourth-order gradient approximation of exchange is important. Both the TM and regTM functional recover the slowly varying fourth-order gradient approximation correctly. In Table I, we have shown the MAE in lattice constants, bulk moduli, and cohesive energies of 29 bulk solids (compiled in ref. [24]) as obtained from TM and regTM functionals. For lattice constants the zero-point an-harmonic expansion (ZPAE) corrected reference values are taken from ref. [36, 46, 49]. It is shown, for accurate functional assessment, one should consider the ZPAE corrected lattice constant values [62]. Regarding the lattice constants performance, TM and regTM perform almost similarly. Both functionals underestimate the lattice constants for metals and ionic solids. Note that solids like Li, Na, and K are also known as “soft matter”, for which the lattice constants is influenced by the short-range part of the vdW interaction [79]. Although,

semilocal density functionals like MS1, MS2, MVS, and SCAN functionals include some amount of short-range part of the vdW interaction [26, 54], none of the TM and regTM functionals incorporate the short-range part of the vdW interaction and their good results solely depends on the error cancellation between exchange and correlation. Note that the correlation part of the TM functional proposed from modified TPSS correlation, which incorporate (i) one-electron self-interaction free correlation, (ii) correct slowly varying density limit of the correlation and local density linear response of the uniform electron gas limit, and (iii) spin independent of the XC functional for  $0 < \zeta < 1$  [28]. The constraint (ii) is only important for the solids, where the error cancellation between XC and restoration of good property of LSDA is important. In this respect the regTPSS correlation functional, used also in regTM functional, keeps the correct formal properties of the solids i.e., correct slowly varying density limit of the correlation. However, only differences in the TM and regTM construction from the lattice constants performance come from error cancellation between exchange and correlation which seems to be a bit better for TM functional, especially, for semiconductor and a few metals. Nevertheless, the performance of the regTM functional can be improved by incorporating a suitable meta-GGA ingredients dependent correlation energy functional compatible with the exchange or by including more exact constraints in the functional form. Overall, for the LC29 test set, we observe MAE of the  $0.036 \text{ \AA}$  from regTM functional compared to the  $0.033 \text{ \AA}$  as obtained from TM functional.

To remark on the functional performance for bulk solids, in Fig. 4 we have shown the variation of  $f(\alpha, p)$ ,  $z$ ,  $z'$ ,  $w$  and  $w'$  for the bulk solid Li (simple metal). The right panel of Fig. 4 shows that inside the bulk solid both the  $w$  and  $w'$  becomes one, while outside bulk both decay to zero, indicating the likeness of the both interpolation parameters. However, a closer look (shown in left panel of Fig. 4) suggests that for the overlap of the closed cell towards the valance region,  $f(\alpha, p)$  and  $z'$  slightly oscillate (also  $w'$ ), which also slightly shrink the lattice con-

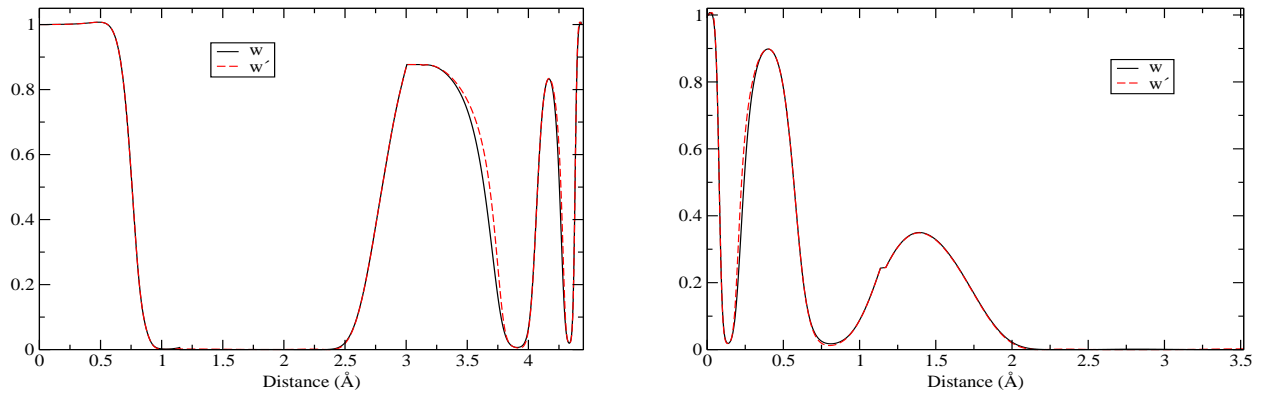


FIG. 5. Shown is the interpolation function  $w$  and  $w'$  for LiCl from the Li atom at  $(0, 0, 0)$  to the Cl atom at  $(1/2, 1/2, 1/2)$  (left panel) and Si from the atom at  $(1/8, 1/8, 1/8)$  to  $(1/2, 1/2, 1/2)$  (right panel).

TABLE II. Tabulated are the phase transition pressure ( $P_t$ ) (in GPa), and energy difference ( $\Delta E_e$ ) (in eV/functional) of highly symmetric phases using TM and regTM functionals. For reference comparison, the ( $\Delta E_e$ ) is compared with SCAN/ ACSEX from ref. [78]. All values are without temperature corrections.

Solids	Expt. <sup>a</sup>	$P_t$		SCAN/ACSEX <sup>a</sup>	$\Delta E_e$	
		TM	regTM		TM	regTM
Si	12.0	3.9	14.5	0.417/0.328	0.246	0.415
Ge	10.6	6.7	7.5	0.265/0.280	0.365	0.394
SiC	100.0	52.5	66.9	1.631/1.599	1.227	1.548
GaAs	15.0	8.2	14.9	0.825/0.978	0.659	0.728
Pb	14.0	10.0	15.08	0.015/0.027	0.007	0.024
C	3.7	2.17	4.81	0.088/0.130	0.040	0.086
BN	5.0	-1.2	1.11	0.105/0.048	0.044	0.042

a) See ref. [78] and all references therein.

stant of Li for regTM. This slightly different behavior of  $w'$  purely coming from  $f(\alpha, p)$  which depends on  $\alpha$ . We also observe similar behavior for LiCl (ionic solid) and Si (semiconductor) (shown in Fig. 5). However, the similar behavior of  $w$  and  $w'$  indicate the judicious choice of  $w'$ . Overall, it correctly recovers  $w$  throughout the range of the slowly varying bulk solids and rapidly or moderately varying atomic region.

Next, we focus on the bulk moduli of the solids. The bulk moduli are obtained from the equation of state fitting of the energy versus volume curve of the unit cell with the third-order Birch-Murnaghan isothermal equation of state. The volume of the unit cell is varied in the range  $V_0 \pm 5\%$ , where  $V_0$  is the equilibrium volume. This test depends on the accuracy of the geometries as predicted by the semilocal functional. As both the TM and regTM are quite good in predicting the geometries, the overall mean absolute errors obtain from both the functionals are about  $\leq 5.5$  GPa. For comparison, we also show the BM20 results which can be directly compared with the results of other functionals presented in refs. [27, 49].

The cohesive energy is also an important property for solids and it is related to the thermodynamics of solids. However, good accuracy for the lattice constants does not guarantee simultaneous good accuracy for cohesive energies. For example in the semilocal level, PBEsol does not

perform as well as its lattice constants prediction for the cohesive energies. In most cases, meta-GGA functionals performance is better than GGA for cohesive energies because of their dependence on the additional ingredient i.e., KS kinetic energy density. For the accurate cohesive energies, simultaneous good performance for valence densities (which is moderately and rapidly varying) of atoms together with the bulk densities (which is slowly varying) is required. The cohesive energy per/atom is calculated as,

$$E_{coh} = E_{atom} - \frac{E_{bulk}}{N}, \quad (15)$$

where  $E_{atom}$  is the atomic energy and  $E_{bulk}$  is the bulk energy of the unit cell having  $N$  atoms.

Our results show that cohesive energies of alkali metals and transition metals are the most challenging for meta-GGA, where GGA PBE generally performs better [52, 80, 81]. For transition metal, the total charge density becomes the sum of the several one-electron orbitals because of the largely filled  $d$  shell. Therefore, the meta-GGA ingredients play a significant role in describing the energetic of the alkali metals [80]. From Table I, we observe that, for alkali metals and transition metals, regTM shows improvement over the TM. Improvement of regTM over TM is also observed for semiconductors. While for ionic solids, TM performs a bit better. The improved

performance of regTM probably due to the slightly improved atomization energies and oscillatory nature of the  $w'$  (and/or exchange enhancement factor) in the valence band of solids and core of the isolated atoms. Overall, regTM describes slightly better the slowly varying density and rapidly or moderately varying atomic region. Note that the SCAN functional also shows similar accuracy [36] (or more accurate) for the 29 test set presented in Table I. Nevertheless, one can not judge the improved performance of regTM from the modification in exchange only, the semilocal correction energy and long-range vdW interactions also play an important roles [80, 82]

Lastly, in this section, we also focus on the TM and regTM performance of the binding energies of Ar<sub>2</sub> dimer and graphite bi-layer. The Ar<sub>2</sub> dimer represents the non-covalent interaction and graphite bi-layer represents the layered materials. These two systems are often important to assess the quality of a functional for non-covalent interactions in molecular and solids level. The regTM binding energy curve a little bit up-shifted than TM functional for both the Ar<sub>2</sub> dimer and graphite bi-layer. This is probably due to the lack of the one-electron self-interaction free correlation. Nevertheless, regTM performs very closely to TM functional for these systems indicating the reliability and closeness of  $w$  and  $w'$ .

### B. Structural phase transition

Accurate prediction of the pressure-induced structural phase transition of solids from low-pressure phases (LP) to high-pressure phases (HP) having practical implication [83–85] and density functional semilocal and higher-order accurate wave functional methods are very successful in predicting the phase transition pressure [78, 86–90]. The accurate phase transition pressure depends on the accurate prediction of the both the equilibrium geometries and energy differences of the LP and HP phases. Regarding the various semilocal approaches, while LDA is good for structural properties, it tends to underestimate the energy difference of two phases [78, 86]. The PBE GGA overestimates the volume and performs better than LDA for energy differences and phase transition pressure [78, 86]. Recent advances in the development of the semilocal functional shows that the meta-GGA functionals like MS1, MS2, MVS and SCAN functionals performs better than PBE in predicting the phases transition pressure [78, 87, 90].

For meta-GGA functionals, the improved phase transition pressure is related to the artifact of the order-of-limit problem [27, 62] which is related to the wrong energy difference between LP and HP phases. The meta-GGA having order-of-limit problem mostly underestimates (also overestimates in a few cases) the energy difference and hence predict the phase transition pressure wrongly, as it is shown for revTPSS functional [27]. The TM functional which also possesses the order-of-limit problem underestimates the phase transition pressure [62]. As state in

TABLE III. Selective semiconductor band gaps (in eV) as obtained from regTM and TM functionals.

Solids	Expt.	TM	regTM
C	5.5	4.08	5.08
Si	1.17	0.56	1.26
Ge	0.74	0.32	0.40
SiC	2.42	1.29	1.75
BP	2.4	1.20	1.94
GaAs	1.52	0.91	1.01

ref. [27], the order-of-limit problem is more severe for covalent bonded solids, where the  $\alpha \approx 0$ , and  $s \approx 0$  often encounter around the critical bond point and shows the wrong energy difference between two phases of solids.

To illustrate the improvement of the phase transition pressure from regTM functional, in Table II, the structural phase transition parameters as obtained from the TM and regTM functional are compared. We observe that the regTM yields phase transition pressure and energy differences close to the experimental one than the TM functional. For Si phase transition, regTM functional predicts improves considerably for energy difference and energy difference of two phases. Comparing the SCAN and ACSOSEX values from ref. [78], the regTM is considerably close to that SCAN, indicating its improvement over TM upon eliminating the order-of-limit problem. A very similar tendency is observed for other structural phase transitions, where regTM improves considerably over TM functional. The regTM phase transition pressure of Si, GaAs, and Pb become very close to the experiment, where TM underestimates considerably. For those solids, the energy difference between the two phases is also close to that of the SCAN/ASCOSEX values [90]. For cubic to hexagonal phase transition of BN, the agreement of phase transition pressure for TM functional is very poor. It shows negative phase transition pressure, where regTM improves considerably over TM. However, we do not include the temperature corrections in our calculations, which as par shows about to improve the phase transition pressure considerably for BN [78].

It is noteworthy to mention that accurate prediction of the phase transition pressure depends both the differences, the energy ( $\Delta E_e$ ) and volume ( $\Delta V_0$ ) differences. While both the functional perform almost similarly for geometries, regTM performs better for energy differences. Therefore, it is clearly indicating that the elimination of the order-of-limit problem is important for the improvement of the structural phase transition properties from the semiconductor to metallic phases.

### C. Connection to the band gap

On eliminating the order-of-limit problem, the regTM functional also improves the semiconductor band gaps. In Table III we have shown the band gaps of few selec-

tive solids for which a clear improvement of regTM over TM is evident. For diamond C, the regTM band gap increases by almost 1 eV. Similarly, for Si, Ge, SiC, BP, and GaAs, we observe the improvement in the band gap of solids. However, this improvement is related to the slope of the exchange enhancement factor which is discussed in ref. [35, 55]. For regTM the slope  $\partial F_x/\partial\alpha$  is more negative, which includes more derivative discontinuity ( $\Delta_{xc}$ ) in the generalized KS scheme [35]. This also happens for functionals like MS1, MS2, MVS, SCAN, MGGAC, and TASK functionals behavior. However, for regTM this happens only for  $\alpha \approx 0$  and  $s \approx 0$  region, relevant for the covalent bonded systems. For other regions, regTM exchange enhancement factor matches closely to that of the TM functional.

Next, we consider the relation between improvement to the phase transition pressure and the band gap, which is discussed in refs. [91, 92]. In ref. [91], it is argued that the underestimation of the phase transition pressure for Si for LDA and GGA may be related to the band gap of solids. While higher order methods like GW and screened hybrid functional HSE06 enhance the density of state (DOS) near Fermi level and describes the covalent bonding more conveniently which may responsible for the improved phase transition pressure for those methods [91]. Contrary to ref. [91], in ref. [92], it is stated that the impact of the fundamental band gap may not be so important for the improvement in the phase transition pressure. However, in this case, the band gap improvement for regTM for semiconductors, especially for Si, indicates that the regTM transition pressures may be related to the improvement to the band gap in Si as suggested in ref. [91].

#### IV. CONCLUSIONS

The order-of-limit problem is an important limitation of the TM functional to predict the phase transition pressure as shown in ref. [62]. In this paper, a modified interpolation function of the Tao-Mo (TM) functional is proposed which resolves the order-of-limit of the TM functional. Using the modified interpolation function, the proposed functional correctly retains the accuracy of the parent functional for one- or two-electron limit, slowly varying density correction, and non-covalent interacting systems. This is important because along with the resolution of the order-of-limit problem, we retain the main functional accuracy for thermochemistry and solid-state physics which are simultaneously important. It is shown that the phase transition pressure of the proposed functional is improved corresponding to the TM functional. As claimed in ref. [62], redesign the interpolation function as a function of  $\alpha$  may also resolve the order-of-limit

problem of the TM functional, but in that case, one has to ensure simultaneous good accuracy of the parent functional. In these prospects, the present modification of the TM functional to make it free from the order-of-limit problem seems quite suitable.

Lastly, we conclude that the present modification of the iso-orbital indicator  $z$  is simple and quite useful as it can be used further to construct meta-GGA functionals development. Along this line of construction, a one-electron self-interaction free correlation with the regTM exchange functional may also enhance the performance of it for several thermochemical and solid-state structural properties. However, this can be further revisited in future publications.

**Computational details:** The molecular calculations of the functionals are performed using the developed version of Q-CHEM code [93] with def2-QZVP basis set (for IP13 and WATER27 the def2-QZVPD basis set is used) with 99 points radial grid and 590 points angular Lebedev grid. Note that like both the TM and regTM functionals are not sensitive on the choice of the grid. Using the 350 points radial grid and 590 points angular Lebedev grid also we do not see any difference in the potential energy curves for non-bonded interactions. Hence, the choice of the more dense grid is not required and the present choice of the grid is quite adequate for the energy convergence.

All solid-state calculations are performed in plane wave suite code *Vienna ab initio simulation package* (VASP) [94–100]. The lattice constants are performed by relaxing the volume and internal co-ordinates using conjugate gradient algorithm. For bulk calculations we used  $20 \times 20 \times 20$   $\Gamma$  centered  $\mathbf{k}$  points with 800 eV energy cutoff. The spin polarized atomic calculation for the cohesive energies are performed with the orthorhombic box of size of  $23 \times 24 \times 25 \text{ \AA}^3$ . To calculate the bulk moduli and phase transition pressure third order Birch-Murnaghan equation of state [101] is used.

#### ACKNOWLEDGEMENTS

S.J. is grateful to the NISER for partial financial support. Q-CHEM and VASP simulations has been performed on *KALINGA* and *NISERDFT* high performance computing facility at NISER, Bhubaneswar. P.S. thanks Q-CHEM Inc. and developers for providing the source code.

#### V. DATA AVAILABILITY

The details of the pseudopotential used in this calculations along with all the results are supplied in the supporting information.

---

[1] P. Hohenberg and W. Kohn, Phys. Rev. **136**, B864 (1964).

[2] W. Kohn and L. J. Sham, Phys. Rev. **140**, A1133 (1965).

- [3] J. P. Perdew and A. Zunger, *Phys. Rev. B* **23**, 5048 (1981).
- [4] J. P. Perdew, K. Burke, and M. Ernzerhof, *Phys. Rev. Lett.* **77**, 3865 (1996).
- [5] R. Armiento and A. E. Mattsson, *Phys. Rev. B* **72**, 085108 (2005).
- [6] Z. Wu and R. E. Cohen, *Phys. Rev. B* **73**, 235116 (2006).
- [7] Y. Zhao and D. G. Truhlar, *J. Chem. Phys.* **128**, 184109 (2008).
- [8] J. P. Perdew, A. Ruzsinszky, G. I. Csonka, O. A. Vydrov, G. E. Scuseria, L. A. Constantin, X. Zhou, and K. Burke, *Phys. Rev. Lett.* **100**, 136406 (2008).
- [9] L. A. Constantin, J. C. Snyder, J. P. Perdew, and K. Burke, *J. Chem Phys.* **133**, 241103 (2010).
- [10] L. A. Constantin, J. P. Perdew, and J. M. Pitarke, *Phys. Rev. B* **79**, 075126 (2009).
- [11] E. Fabiano, L. A. Constantin, P. Cortona, and F. Della Sala, *J. Chem. Theory Comput.* **11**, 122 (2014).
- [12] L. A. Constantin, L. Chiodo, E. Fabiano, I. Bodrenko, and F. D. Sala, *Phys. Rev. B* **84**, 045126 (2011).
- [13] E. Fabiano, L. A. Constantin, and F. Della Sala, *J. Chem. Theory Comput.* **7**, 3548 (2011).
- [14] L. A. Constantin, *Phys. Rev. B* **93**, 121104 (2016).
- [15] L. A. Constantin, A. Terentjevs, F. Della Sala, P. Cortona, and E. Fabiano, *Phys. Rev. B* **93**, 045126 (2016).
- [16] A. Cancio, G. P. Chen, B. T. Krull, and K. Burke, *J. Chem. Phys.* **149**, 084116 (2018).
- [17] L. Chiodo, L. A. Constantin, E. Fabiano, and F. Della Sala, *Phys. Rev. Lett.* **108**, 126402 (2012).
- [18] A. D. Becke and M. R. Roussel, *Phys. Rev. A* **39**, 3761 (1989).
- [19] T. Van Voorhis and G. E. Scuseria, *J. Chem. Phys.* **109**, 400 (1998).
- [20] Y. Zhao and D. G. Truhlar, *J. Chem. Phys.* **125**, 194101 (2006).
- [21] J. P. Perdew, S. Kurth, A. c. v. Zupan, and P. Blaha, *Phys. Rev. Lett.* **82**, 2544 (1999).
- [22] J. Tao, J. P. Perdew, V. N. Staroverov, and G. E. Scuseria, *Phys. Rev. Lett.* **91**, 146401 (2003).
- [23] J. P. Perdew, A. Ruzsinszky, G. I. Csonka, L. A. Constantin, and J. Sun, *Phys. Rev. Lett.* **103**, 026403 (2009).
- [24] L. A. Constantin, E. Fabiano, and F. D. Sala, *Phys. Rev. B* **86**, 035130 (2012).
- [25] L. A. Constantin, E. Fabiano, and F. Della Sala, *J. Chem. Theory Comput.* **9**, 2256 (2013).
- [26] J. Sun, A. Ruzsinszky, and J. P. Perdew, *Phys. Rev. Lett.* **115**, 036402 (2015).
- [27] A. Ruzsinszky, J. Sun, B. Xiao, and G. I. Csonka, *J. Chem. Theory Comput.* **8**, 2078 (2012).
- [28] J. Tao and Y. Mo, *Phys. Rev. Lett.* **117**, 073001 (2016).
- [29] Y. Wang, X. Jin, H. S. Yu, D. G. Truhlar, and X. He, *Proc. Natl. Acad. Sci. U. S. A.* **114**, 8487 (2017).
- [30] P. D. Mezei, G. I. Csonka, and M. Kllay, *J. Chem. Theory Comput.* **14**, 2469 (2018).
- [31] F. Della Sala, E. Fabiano, and L. A. Constantin, *Int. J. Quantum Chem.* **116**, 1641.
- [32] J. W. Furness and J. Sun, *Phys. Rev. B* **99**, 041119 (2019).
- [33] J. Sun, B. Xiao, and A. Ruzsinszky, *The Journal of Chemical Physics* **137**, 051101 (2012).
- [34] J. Sun, R. Haunschild, B. Xiao, I. W. Bulik, G. E. Scuseria, and J. P. Perdew, *The Journal of Chemical Physics* **138**, 044113 (2013).
- [35] T. Aschebrock and S. Kümmel, *Phys. Rev. Research* **1**, 033082 (2019).
- [36] S. Jana, K. Sharma, and P. Samal, *J. Phys. Chem. A* **123**, 6356 (2019).
- [37] L. A. Constantin, E. Fabiano, J. M. Pitarke, and F. Della Sala, *Phys. Rev. B* **93**, 115127 (2016).
- [38] B. Patra, S. Jana, L. A. Constantin, and P. Samal, *Phys. Rev. B* **100**, 155140 (2019).
- [39] J. Heyd, G. E. Scuseria, and M. Ernzerhof, *The Journal of chemical physics* **118**, 8207 (2003).
- [40] .
- [41] S. Jana, A. Patra, L. A. Constantin, and P. Samal, *The Journal of Chemical Physics* **152**, 044111 (2020), <https://doi.org/10.1063/1.5131530>.
- [42] V. N. Staroverov, G. E. Scuseria, J. Tao, and J. P. Perdew, *J. Chem. Phys.* **119**, 12129 (2003).
- [43] L. Goerigk and S. Grimme, *J. Chem. Theory Comput.* **7**, 291 (2011).
- [44] P. Hao, J. Sun, B. Xiao, A. Ruzsinszky, G. I. Csonka, J. Tao, S. Glindmeyer, and J. P. Perdew, *J. Chem. Theory Comput.* **9**, 355 (2013).
- [45] Y. Mo, G. Tian, and J. Tao, *Phys. Chem. Chem. Phys.* **19**, 21707 (2017).
- [46] P. Haas, F. Tran, and P. Blaha, *Phys. Rev. B* **79**, 085104 (2009).
- [47] F. Tran, J. Stelzl, and P. Blaha, *J. Chem. Phys.* **144**, 204120 (2016).
- [48] Y. Mo, R. Car, V. N. Staroverov, G. E. Scuseria, and J. Tao, *Phys. Rev. B* **95**, 035118 (2017).
- [49] J. Sun, M. Marsman, G. I. Csonka, A. Ruzsinszky, P. Hao, Y.-S. Kim, G. Kresse, and J. P. Perdew, *Phys. Rev. B* **84**, 035117 (2011).
- [50] G. I. Csonka, J. P. Perdew, A. Ruzsinszky, P. H. T. Philipsen, S. Lebègue, J. Paier, O. A. Vydrov, and J. G. Ángyán, *Phys. Rev. B* **79**, 155107 (2009).
- [51] S. Jana, A. Patra, and P. Samal, *J. Chem. Phys.* **149**, 044120 (2018).
- [52] S. Jana, K. Sharma, and P. Samal, *J. Chem. Phys.* **149**, 164703 (2018).
- [53] A. Patra, J. E. Bates, J. Sun, and J. P. Perdew, *Proc. Natl. Acad. Sci. U. S. A.* **114**, E9188 (2017).
- [54] J. Sun, B. Xiao, Y. Fang, R. Haunschild, P. Hao, A. Ruzsinszky, G. I. Csonka, G. E. Scuseria, and J. P. Perdew, *Phys. Rev. Lett.* **111**, 106401 (2013).
- [55] A. Patra, B. Patra, L. A. Constantin, and P. Samal, *Phys. Rev. B* **102**, 045135 (2020).
- [56] B. Patra, S. Jana, L. A. Constantin, and P. Samal, *Phys. Rev. B* **100**, 045147 (2019).
- [57] J. Sun, R. C. Remsing, Y. Zhang, Z. Sun, A. Ruzsinszky, H. Peng, Z. Yang, A. Paul, U. Waghmare, X. Wu, M. L. Klein, and J. P. Perdew, *Nat. Chem.* **8**, 831 (2016).
- [58] B. Patra, S. Jana, and P. Samal, *Phys. Chem. Chem. Phys.* **20**, 8991 (2018).
- [59] S. Jana and P. Samal, *Phys. Chem. Chem. Phys.* **20**, 8999 (2018).
- [60] S. Jana and P. Samal, *Phys. Chem. Chem. Phys.* **21**, 3002 (2019).
- [61] S. Jana, B. Patra, H. Myneni, and P. Samal, *Chemical Physics Letters* **713**, 1 (2018).
- [62] J. W. Furness, N. Sengupta, J. Ning, A. Ruzsinszky, and J. Sun, *The Journal of Chemical Physics* **152**, 244112 (2020), <https://doi.org/10.1063/5.0008014>.

- [63] J. P. Perdew, J. Tao, V. N. Staroverov, and G. E. Scuseria, *The Journal of Chemical Physics* **120**, 6898 (2004), <https://doi.org/10.1063/1.1665298>.
- [64] S. Jana, L. A. Constantin, and P. Samal, *Journal of Chemical Theory and Computation* **16**, 974 (2020), pMID: 31910012, <https://doi.org/10.1021/acs.jctc.9b01018>.
- [65] K. Patkowski, G. Murdachaew, C.-M. Fou, and K. S. \*, *Molecular Physics* **103**, 2031 (2005), <https://doi.org/10.1080/00268970500130241>.
- [66] P. Slavek, R. Kalus, P. Paka, I. Odvrkov, P. Hobza, and A. Malijevsk, *The Journal of Chemical Physics* **119**, 2102 (2003), <https://doi.org/10.1063/1.1582838>.
- [67] T. Björkman, A. Gulans, A. V. Krasheninnikov, and R. M. Nieminen, *Phys. Rev. Lett.* **108**, 235502 (2012).
- [68] R. Peverati and D. G. Truhlar, *Philosophical Transactions of the Royal Society A: Mathematical, Physical and Engineering Sciences* **372**, 20120476 (2014), <https://royalsocietypublishing.org/doi/pdf/10.1098/rsta.20120476>.
- [69] V. S. Bryantsev, M. S. Diallo, A. C. T. van Duin, and W. A. Goddard, *J. Chem. Theory Comput.* **5**, 1016 (2009).
- [70] D. Manna, M. K. Kesharwani, N. Sylvetsky, and J. M. L. Martin, *J. Chem. Theory Comput.* **13**, 3136 (2017).
- [71] L. A. Curtiss, K. Raghavachari, P. C. Redfern, and J. A. Pople, *The Journal of Chemical Physics* **106**, 1063 (1997).
- [72] L. Goerigk, A. Hansen, C. Bauer, S. Ehrlich, A. Najibi, and S. Grimme, *Phys. Chem. Chem. Phys.* **19**, 32184 (2017).
- [73] B. J. Lynch and D. G. Truhlar, *The Journal of Physical Chemistry A* **108**, 1460 (2004), <https://doi.org/10.1021/jp0379190>.
- [74] Y. Zhao and D. G. Truhlar, *Journal of Chemical Theory and Computation* **1**, 415 (2005).
- [75] Y. Zhao and D. G. Truhlar, *The Journal of Physical Chemistry A* **109**, 5656 (2005).
- [76] P. Jurecka, J. Spöner, J. Cerny, and P. Hobza, *Phys. Chem. Chem. Phys.* **8**, 1985 (2006).
- [77] M. S. Marshall, L. A. Burns, and C. D. Sherrill, *The Journal of Chemical Physics* **135**, 194102 (2011).
- [78] N. Sengupta, J. E. Bates, and A. Ruzsinszky, *Phys. Rev. B* **97**, 235136 (2018).
- [79] J. Tao, J. P. Perdew, and A. Ruzsinszky, *Phys. Rev. B* **81**, 233102 (2010).
- [80] L. Schimka, R. Gaudoin, J. c. v. Klimeš, M. Marsman, and G. Kresse, *Phys. Rev. B* **87**, 214102 (2013).
- [81] P. Kovcs, F. Tran, P. Blaha, and G. K. H. Madsen, *The Journal of Chemical Physics* **150**, 164119 (2019), <https://doi.org/10.1063/1.5092748>.
- [82] J. Tao, F. Zheng, J. Gebhardt, J. P. Perdew, and A. M. Rappe, *Phys. Rev. Materials* **1**, 020802 (2017).
- [83] V. K. Vlasko-Vlasov, Y. K. Lin, D. J. Miller, U. Welp, G. W. Crabtree, and V. I. Nikitenko, *Phys. Rev. Lett.* **84**, 2239 (2000).
- [84] Y. Kang, S. Najmaei, Z. Liu, Y. Bao, Y. Wang, X. Zhu, N. J. Halas, P. Nordlander, P. M. Ajayan, J. Lou, and Z. Fang, *Advanced Materials* **26**, 6467 (2014), <https://onlinelibrary.wiley.com/doi/pdf/10.1002/adma.201401802>.
- [85] A. Kato, M. Nishigaki, N. Mamedov, M. Yamazaki, S. Abdullayeva, E. Kerimova, H. Uchiki, and S. Iida, *Journal of Physics and Chemistry of Solids* **64**, 1713 (2003), 13th International Conference on Ternary and Ternary Compounds.
- [86] N. Moll, M. Bockstedte, M. Fuchs, E. Pehlke, and M. Scheffler, *Phys. Rev. B* **52**, 2550 (1995).
- [87] B. Xiao, J. Sun, A. Ruzsinszky, J. Feng, and J. P. Perdew, *Phys. Rev. B* **86**, 094109 (2012).
- [88] H.-J. Kim, S.-H. Kang, I. Hamada, and Y.-W. Son, *Phys. Rev. B* **95**, 180101 (2017).
- [89] F. El-Mellouhi, E. N. Brothers, M. J. Lucero, I. W. Bulik, and G. E. Scuseria, *Phys. Rev. B* **87**, 035107 (2013).
- [90] C. Shahi, J. Sun, and J. P. Perdew, *Phys. Rev. B* **97**, 094111 (2018).
- [91] R. G. Hennig, A. Wadehra, K. P. Driver, W. D. Parker, C. J. Umrigar, and J. W. Wilkins, *Phys. Rev. B* **82**, 014101 (2010).
- [92] B. Xiao, J. Sun, A. Ruzsinszky, J. Feng, R. Haunschuld, G. E. Scuseria, and J. P. Perdew, *Phys. Rev. B* **88**, 080401 (2013).
- [93] W. Shao, Z. Gan, E. Epifanovsky, A. T. Gilbert, M. Wormit, J. Kussmann, A. W. Lange, A. Behn, J. Deng, X. Feng, D. Ghosh, M. Goldey, P. R. Horn, L. D. Jacobson, I. Kaliman, R. Z. Khaliullin, T. Ku, A. Landau, J. Liu, E. I. Proynov, Y. M. Rhee, R. M. Richard, M. A. Rohrdanz, R. P. Steele, E. J. Sundstrom, H. L. W. III, P. M. Zimmerman, D. Zuev, B. Albrecht, E. Alguire, B. Austin, G. J. O. Beran, Y. A. Bernard, E. Berquist, K. Brandhorst, K. B. Bravaya, S. T. Brown, D. Casanova, C.-M. Chang, Y. Chen, S. H. Chien, K. D. Closser, D. L. Crittenden, M. Diedenhofen, R. A. D. Jr., H. Do, A. D. Dutoi, R. G. Edgar, S. Fatehi, L. Fusti-Molnar, A. Ghysels, A. Golubeva-Zadorozhnaya, J. Gomes, M. W. Hanson-Heine, P. H. Harbach, A. W. Hauser, E. G. Hohenstein, Z. C. Holden, T.-C. Jagau, H. Ji, B. Kaduk, K. Khistyayev, J. Kim, J. Kim, R. A. King, P. Klunzinger, D. Kosenkov, T. Kowalczyk, C. M. Krauter, K. U. Lao, A. D. Laurent, K. V. Lawler, S. V. Levchenko, C. Y. Lin, F. Liu, E. Livshits, R. C. Lochan, A. Luenser, P. Manohar, S. F. Manzer, S.-P. Mao, N. Mardirossian, A. V. Marenich, S. A. Maurer, N. J. Mayhall, E. Neuscamman, C. M. Oana, R. Olivares-Amaya, D. P. O'Neill, J. A. Parkhill, T. M. Perrine, R. Peverati, A. Prociuk, D. R. Rehn, E. Rosta, N. J. Russ, S. M. Sharada, S. Sharma, D. W. Small, A. Sodt, T. Stein, D. Stck, Y.-C. Su, A. J. Thom, T. Tsuchimochi, V. Vanovschi, L. Vogt, O. Vydrov, T. Wang, M. A. Watson, J. Wenzel, A. White, C. F. Williams, J. Yang, S. Yeganeh, S. R. Yost, Z.-Q. You, I. Y. Zhang, X. Zhang, Y. Zhao, B. R. Brooks, G. K. Chan, D. M. Chipman, C. J. Cramer, W. A. G. III, M. S. Gordon, W. J. Hehre, A. Klamt, H. F. S. III, M. W. Schmidt, C. D. Sherrill, D. G. Truhlar, A. Warshel, X. Xu, A. Aspuru-Guzik, R. Baer, A. T. Bell, N. A. Besley, J.-D. Chai, A. Dreuw, B. D. Dunietz, T. R. Furlani, S. R. Gwaltney, C.-P. Hsu, Y. Jung, J. Kong, D. S. Lambrecht, W. Liang, C. Ochsenfeld, V. A. Ras-solov, L. V. Slipchenko, J. E. Subotnik, T. V. Voorhis, J. M. Herbert, A. I. Krylov, P. M. Gill, and M. Head-Gordon, *Molecular Physics* **113**, 184 (2015).
- [94] G. Kresse and J. Furthmüller, *Phys. Rev. B* **54**, 11169 (1996).
- [95] G. Kresse and D. Joubert, *Phys. Rev. B* **59**, 1758 (1999).
- [96] G. Kresse and J. Furthmüller, *Computational Materials Science* **6**, 15 (1996).

- [97] G. Kresse and J. Hafner, Phys. Rev. B **47**, 558 (1993).  
[98] G. Kresse and J. Hafner, Phys. Rev. B **49**, 14251 (1994).  
[99] G. Kresse and J. Hafner, Phys. Rev. B **48**, 13115 (1993).  
[100] G. Kresse and J. Hafner, Journal of Physics: Condensed Matter **6**, 8245 (1994).  
[101] F. Birch, Phys. Rev. **71**, 809 (1947).